

**WCCE-ECCE-TCCE Joint Conference 2**  
**Seismic Protection of Cultural Heritage**  
**October 31-November 1, 2011, Antalya, Turkey**

---

## **DYNAMIC IDENTIFICATION AND MONITORING OF CULTURAL HERITAGE BUILDINGS**

**Paulo B. Lourenço<sup>\*</sup>, Luís F. Ramos<sup>\*\*</sup>**

### **ABSTRACT**

*Preservation of architectural heritage is considered a fundamental issue in the cultural life of modern societies. This heritage is accumulating damage due to deterioration of materials, repeated loading and exceptional events. This means that conservation, repair and strengthening are often necessary. In this process, monitoring and non-destructive testing play a major role, providing information on the building condition and existing damage, and allowing to define adequate remedial measures. Dynamic based methods are an attractive tool because they are non-destructive and are able to capture the global structural behavior. The present paper focuses on three main aspects related to dynamic identification and monitoring: (a) exploring damage in masonry structures at an early stage by vibration measurements, using one arch model constructed in the laboratory. Progressive damage was induced in the arch and sequential modal identification analysis was performed at each damage stage, aiming at finding adequate correspondence between dynamic behavior and internal crack growth. The dynamic based methods allowed detecting and locating the damage; (b) two complex case studies of modal and structural identification of monuments using conventional sensors. Operational modal analysis was used to estimate the modal parameters, followed by statistical analysis to evaluate the environmental effects on the dynamic response. The aim is to explore damage assessment in masonry structures at an early stage by vibration signatures, as a part of a health monitoring process; (c) finally, a comparison between commercial wireless based platforms and conventional wired based systems is presented for a laboratory specimen and a structural element from a 15<sup>th</sup> century building.*

---

<sup>\*</sup> Professor, ISISE, Department of Civil Engineering, University of Minho, Azurém, Portugal. Email: [pbl@civil.uminho.pt](mailto:pbl@civil.uminho.pt)

<sup>\*\*</sup> Assistant Professor, ISISE, Department of Civil Engineering, University of Minho, Azurém, Portugal. Email: [ramos@civil.uminho.pt](mailto:ramos@civil.uminho.pt)

## INTRODUCTION

Structural monitoring and damage identification at the earliest possible stage are issues that receive much attention from scientific community. Damage identification is relevant to all the engineering fields as the service loads and the accidental actions may cause damage to the structural systems, Doebling *et al.* (1996). Regular inspections and condition assessment of engineering structures allow programmed repair works and cost-effective management of the infrastructures. In the case of historical constructions, maintenance is even more relevant because of their cultural importance, the safety of visitors, the potential seismic vulnerability and the accumulation of physical, chemical and mechanical damage through time. Dynamic based damage identification methods are based on changes of dynamic parameters (eigen frequencies, mode shapes and damping coefficients), typically a decrease in stiffness and an increasing in damping. As damage is a local phenomenon and may not influence significantly the lower frequencies or the global response, it is important to estimate higher modes and to have accurate information about modal displacements. For these reasons, the methods based on changes on the mode shapes or modal curvatures (or the combination of all responses, e.g. frequencies, modes shapes and modal curvatures) are usually more successful.

The difficulty is to measure accurately the modal strains (modal curvatures) in civil engineering structures or to derivate accurately the modal curvatures from the modal displacements. In any case, to estimate damage a sufficient number of measuring points is necessary in order to have enough spatial resolution of the mode shapes. Historical masonry structures have a complex geometry and successive past interventions, while the constituting materials tend to exhibit significant variations in properties and internal structure. Therefore, the selection of appropriate models for structural analysis is not easy, Lourenço *et al.* (2002, 2007, 2010). Damage in masonry structures are mainly cracks, material deterioration and excessive deformations. When cracks occur, generally they are localized, splitting the structures in macro-blocks. The use of dynamic based methods to identify the damage is an attractive tool to use in this type of structures due to the assumption that damage can be associated with the decrease of stiffness. Many methods are presented in the literature for damage identification based on vibration signatures, but there are relatively few works discussing their application to masonry structures. From the point of view of the applicability of dynamic based identification methods to masonry structures, the aspects under consideration are the possibilities of detection (Level 1), localization (Level 2) and assessment (Level 3). A detailed comparison and a description of different methods are presented elsewhere, Ramos (2007).

The current practices of structural health condition are based mainly on periodic visual inspections or condition surveys but, during the last decade, software and hardware developments made continuous monitoring possible, Chang *et al.* (2003). Typically, one can install hundreds of sensors in a structure and read the data in real time. The attention now seems to be focused on what type of information is important from the structural point of view and how the data should be processed and stored for damage analysis, Maeck (2003). The developments in Micro Electro

Mechanical Systems (MEMS) and Wireless Sensor Networks (WSN) are promising technologies in this field, in particular for historical masonry structures, Lynch (2007) and Ramos *et al.* (2010c), which are also addressed here.

## DAMAGE DETECTION OF ARCHED MASONRY STRUCTURES

The approach used here for arched masonry structures will be based on the modal information estimated by output-only methods. In particular, Stochastic Subspace Identification (SSI) techniques, are among the most robust techniques available for output-only modal identification, see Peeters (2000). These techniques require that excitations are reasonably random in time and in the physical space of the structures, or if excitations are local they must provide sufficient energy to excite the entire structure.

At the moment, there is no unique damage method based on vibration signatures that seems to give accurate results for all levels of damage and for all types of structural systems. Here, a group of methods was selected with two aims: (a) to evaluate the applicability of the methods to masonry structures; (b) to obtain a general perspective of the problem and to provide conclusions on damage identification, taking into account that different methods might provide different results. It is expected that if reasonable damage is present in the structure, the results provided from different methods would converge in the identification, giving more confidence to the analyst. The existence of a group of complementary methods should be understood as an added value in capturing difficult phenomena and in assisting the decision process.

In order to evaluate damage identification methods, one replica of an old masonry arch was built in the laboratory and several controlled Damage Scenarios (DS) were induced with static tests, see Figure 1. For each DS, system identification tests were carried out with SSI techniques and the results of the damage identification methods were compared with the internal crack growth. The ambient temperature and humidity were also recorded, to evaluate possible environmental effects on the dynamic response.

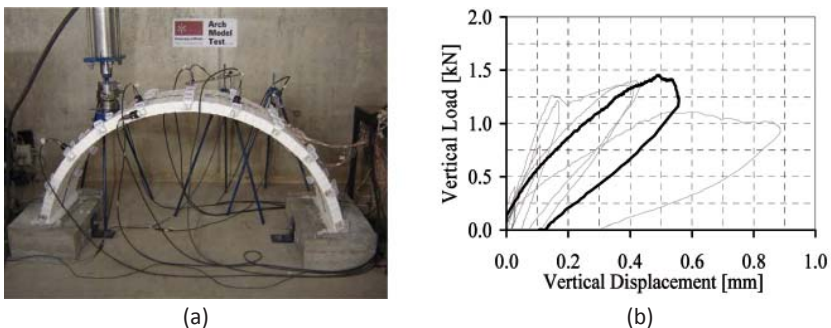


**Figure 1** Arch static tests: (a) view of the test apparatus; (b) example of one damage scenario considered

The arch was built with clay bricks with  $100 \times 50 \times 25 \text{ mm}^3$ , handmade in the northern area of Portugal. The clay bricks have low compressive strength and are laid using a Mapei® mortar with low mechanical properties, trying to be representative of the materials used in historical constructions. The arch has a semicircular shape with a radius of 0.77 m. It has a span equal to 1.50 m, a width equal to 0.45 m, and a thickness equal to 0.05 m. The thickness of the joints is about 0.5 cm. The arch rests in two concrete abutments fixed to the ground floor with bolts, see Ramos et al. (2010a) for more details.

### Static Tests to Induce Damage

The load stages/DS were produced with the application of a static point load located at a quarter span, where the lowest safety factor for arches is obtained. The load was applied with increasing magnitude, being removed after each DS. This assumption tries to represent the situation of temporary exceptional loading in the lifetime of the structure (e.g. a heavy truck passing in a bridge or an earthquake) and assumes that cracks can partially close after the extreme event. The assumption makes the task of damage identification more difficult but more challenging, considering that damage can be difficult to detect with a visual inspection. All the tests were carried out in a period of three months, after 60 days curing.

Figure 1b shows the response of the model during the successive static tests after the first crack, and one selected damage scenario. The tests results in terms of load displacement diagrams indicate a clear loss of stiffness upon reloading, with visible load drops due to crack opening. Figure 2 presents the resulting crack patterns in the arch and the position of the dynamic transducers. Four cracks were found but it was impossible to register the full crack sequence. The first crack to appear (c1) was located between the positions P3 and P4 (accelerometers A03 and A04) and not below the load application point. The crack appears in the intrados, as expected, but it was only visible during the loading branch of the DSVI, although it is evident that it has occurred on DSV, given the loss of stiffness in the static tests.

Crack c2 was located in position P11 (right support in the measuring point A11) in the intrados, crack c3 was located between P8 and P9 (measuring point A08 and

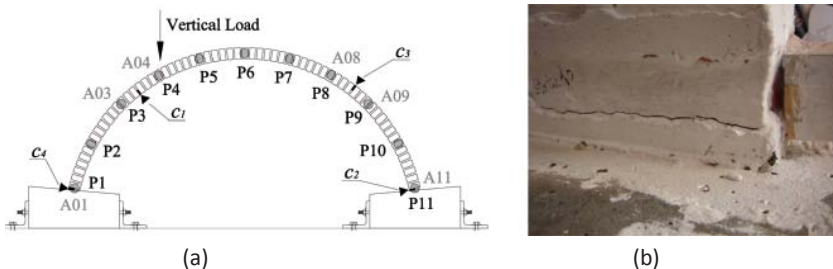


**Figure 2** Arch damage: (a) crack locations (ci) and accelerometer positions (A0i); (b) example of one crack.

A09) in the extrados, and crack c4 was located at position P1 (left support in the measuring point A01) in the extrados, see Figure 2. The load value corresponding to the occurrence of these cracks was impossible to detect. The cracks became visible in the loading range of DSVIII. This can be explained by the fact that the self-weight of the arch is a stabilizing action and almost fully closes the cracks at the equilibrium position. The decision to stop each static test after DSV was based on the sound of a crack that suddenly opens. Therefore, the designation c1 to c4 presented here does not try to represent the real crack sequence, which is partly unknown.

It should be stressed that the maximum remaining crack opening after the entire testing program was 0.05 mm and the maximum crack depth in the loading branch of the tests was 30 mm (more than half of the arch thickness) for crack c1. Analyzing in detail the stiffness during the several load steps presented in Figure 3, after the occurrence of the crack c1 it was possible to observe a decrease of stiffness. A loading and unloading stiffness can be defined, where static tests allow measuring the rapidly varying loading stiffness  $k_l$  and the dynamic tests only measure the slowly varying unloading stiffness  $k_u$ . As a result, dynamic tests are less sensitive than static tests to identify structural damage.

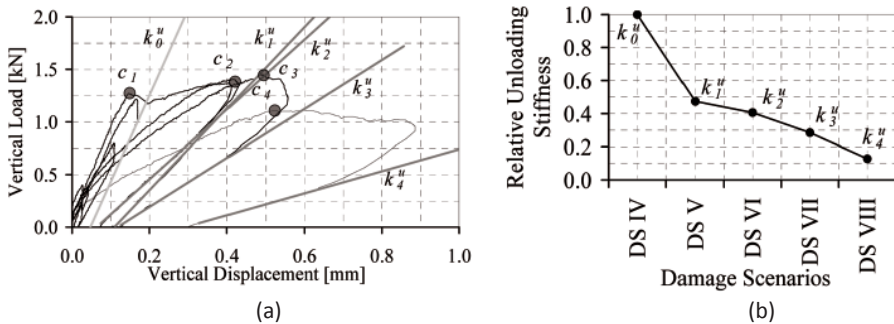


**Figure 3** Stiffness decrease: (a) possible sequence of cracks and gradual stiffness decrease; (b) relative unloading stiffness variation.

### Dynamic Identification Tests

The selected sensors for the dynamic tests were accelerometers and strain gauges. The accelerometers were selected because they have good accuracy for the dynamic response. The strain gauges were chosen to measure directly dynamic strains for the direct estimation of modal curvatures, more sensitive to damage than modal displacements. Another obvious reason is to have more modal information for the damage identification analysis.

From a preliminary numerical analysis to study the test planning, it was possible to conclude that the first twelve modes have significant modal displacements in the

arch plane. In the out-of-plane direction only the numerically predicted 2<sup>nd</sup> and 5<sup>th</sup> modes have significant modal displacements. For this reason, it was decided to measure accelerations only in the in-plane direction, and, for convenience, in the normal and tangential directions on each location. It was also decided to measure both edges of the arch (front and back edges) to estimate the torsion modes and to detect any asymmetric behavior.

According to the configuration of the twelve numerical mode shapes, the best points for the reference transducers (points which have significant modal displacements in all modes) is at  $\frac{1}{4}$  span for some modes and at  $\frac{1}{2}$  span for other modes. In order to have a better resolution in the modal estimation, two positions were selected to be the reference points for accelerations in the front and back edges (four sensors) and four strain gauges in the extrados and intrados (eight sensors). Figure 4 shows the location of the measuring points where the reference points are given in a grey box. The designation  $A_i$  is for accelerometers and  $S_i$  is for strain gauges. In the case of the strain gauges, as an attempt to study the possibility to measure strains for dynamic modal analysis, it was decided to measure only the middle line of the arch on both sides. This means that the torsion modes will not be present in the strains measurements.

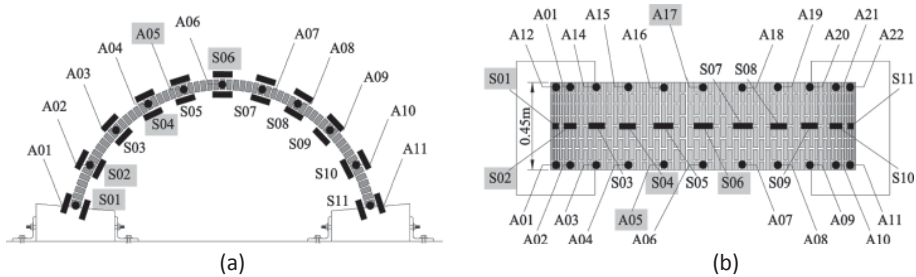


**Figure 4** Location of the measuring points for the dynamic tests: (a) front view; and (b) top view.  $A_i$  indicates accelerometers and  $S_i$  indicates strain gauges. Boxed-values in grey are the reference points.

The dynamic acquisition system was composed by 8 uniaxial piezoelectric accelerometers and 22 strain gauges glued in the masonry. Modal identification tests at each load stage/DS were carried out by two different excitation types: (a) natural and ambient noise present in the laboratory; (b) random impact excitation in space and in time (not recorded), induced by a hammer with 2.5 kg of mass.

The results in terms of frequency values and damping coefficients for the Reference Scenario (RS) are presented in Table 1 for the ambient and random excitation tests, respectively. Both standard deviation ( $\sigma$ ) and Coefficient of Variation (CV) are presented for the same modal parameters: frequency  $\omega$  and damping  $\xi$ . In general, the random impact excitation tests have lower standard deviation values, indicating a possible better modal estimation. Nevertheless, the high CV values for the damping in all cases should be stressed as possible less accurate results. The

**Table 1** Results from the Reference Scenario.

Modes	Ambient Excitation						Random Impact Excitation					
	$\omega$	$\sigma_\omega$	$CV_\omega$	$\xi$	$\sigma_\xi$	$CV_\xi$	$\omega$	$\sigma_\omega$	$CV_\omega$	$\xi$	$\sigma_\xi$	$CV_\xi$
	[Hz]	[Hz]	[%]	[%]	[%]	[%]	[Hz]	[Hz]	[%]	[%]	[%]	[%]
1	35.59	0.20	0.57	0.44	0.20	45.18	35.21	0.12	0.33	0.51	0.08	15.94
2	67.30	0.46	0.69	0.53	0.12	22.50	66.58	0.36	0.55	0.64	0.09	14.68
3	72.11	0.38	0.53	0.88	0.90	101.92	71.16	0.21	0.30	0.72	0.14	19.21
4	125.74	0.65	0.52	0.59	0.10	17.53	124.52	0.74	0.60	0.79	0.10	12.32
5	140.08	0.89	0.63	0.46	0.31	66.76	138.94	0.90	0.65	0.73	0.22	30.11
6	173.38	1.63	0.94	0.83	0.33	39.02	172.54	0.84	0.49	1.11	0.30	27.38
7	199.32	2.91	1.46	1.84	0.65	35.39	196.76	2.13	1.08	2.55	0.94	36.98

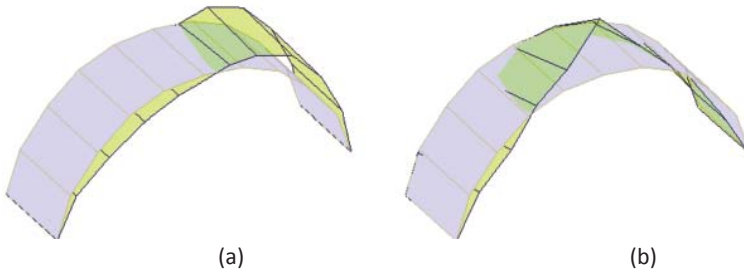


**Figure 5** First mode shape configurations for the undamaged scenarios: (a) mode 1; (b) mode 2.

damping values depend on the excitation and incorporate nonlinear phenomena, but one can conclude that an average value of 0.6% can be observed for all modes and all analyses.

The first modes shapes according to the excitation type are presented in Figure 5, see Ramos et al. (2010a) for more results. All the modes have torsion components, with the exception of the first mode, which has only components in the arch plan. It is stressed that the modes from the two excitation types are highly coincident, with the exception for the modal configuration of the seventh mode shape at middle span and at the left support.

**Experimental Damage Identification Analysis**

The damage analysis over the eight experimental DS induced by increasing external loading is now described. Table 2 presents for the first four estimated modes and for the case of ambient excitation the frequency results for the consecutive DS. The frequency values are presented together with the value  $\pm 2\sigma_\omega$  as a 95% confidence interval, and the frequency differences  $\Delta\omega$  to the RS. It is stressed that small increases in the frequency values are found before the occurrence of the first crack.

**Table 2** Frequency results for the arch model with ambient excitation.

Damage Scenario	Mode 1			Mode 2			Mode 3			Mode 4		
	$\omega$	$2\sigma_\omega$	$\Delta_\omega$	$\omega$	$2\sigma_\omega$	$\Delta_\omega$	$\omega$	$2\sigma_\omega$	$\Delta_\omega$	$\omega$	$2\sigma_\omega$	$\Delta_\omega$
	[Hz]	[Hz]	[Hz]	[Hz]	[Hz]	[Hz]	[Hz]	[Hz]	[Hz]	[Hz]	[Hz]	[Hz]
RS	35.59	0.40	-	67.30	0.93	-	72.11	0.76	-	125.74	1.30	-
DS <sub>I</sub>	35.55	0.31	-0.05	67.51	0.83	0.21	71.80	0.38	-0.30	125.69	1.91	-0.05
DS <sub>II</sub>	35.55	0.24	-0.04	67.39	1.11	0.09	71.83	1.06	-0.28	125.79	2.03	0.05
DS <sub>III</sub>	35.42	0.31	-0.17	67.47	1.19	0.17	71.66	0.94	-0.45	125.75	2.21	0.01
DS <sub>IV</sub>	35.15	0.24	-0.44	67.11	0.88	-0.19	71.33	0.58	-0.78	126.01	1.09	0.28
DS <sub>V</sub> <sup>+</sup>	33.72	0.32	-1.87	65.68	0.72	-1.62	69.36	0.60	-2.75	124.48	1.60	-1.25
DS <sub>VI</sub>	33.19	0.34	-2.40	64.91	1.02	-2.39	68.56	0.58	-3.55	123.58	1.37	-2.16
DS <sub>VII</sub>	31.49	0.44	-4.10	63.08	1.29	-4.22	65.72	0.69	-6.39	121.97	1.83	-3.77
DS <sub>VIII</sub>	28.09	0.62	-7.50	58.44	1.40	-8.86	62.61	0.93	-9.50	119.44	1.76	-6.30

\* - Damage scenario in which the first crack was detected in the static tests.

This is due to the normal adjustments of the structure with the applied load, mainly at the supports and masonry joints. Considering the first four estimated frequencies, the first significant frequency decrease, i.e. higher than  $2\sigma\omega$  (given in a grey box), happens around DSV. In fact, the first significant change in the static stiffness also appears in this scenario. In the subsequent scenarios it is also possible to observe significant frequency decreases.

Figure 6 presents the variation for the frequency, where it is noticeable that damage was detected in DSV and it is coincident with the significant decrease observed in the static results. As a Level 1 approach, the results of the USI method presented in Figure 7 shows the comparison. One conclusion is the difference in the order of values before and after DSV, confirming the significant change that happened in this scenario. The USI values in DSVI are similar to DSV but the last two DS show a significant increase. These results indicate that when the USI is calculated for the several scenarios, the detection of damage (Level 1) is possible. When no information exists about the modal history, the detection of damage with USI might be difficult, because there are no reference values in the undamaged condition.

The analyses carried out with modal displacements were inconclusive, as no damage location is indicated. Using the measured modal curvatures at the middle line of the arch, several methods provided reliable results. Figure 8 presents the results for the relative comparison between DSIV and DSV, where damage occurs at positions P1 and P11 for the Changes in Flexibility Matrix method (CFM) for modal curvatures, and damage occurs at position P1 and P7 for the Sum of all Curvature Errors (SCE) method.

Considering the different observations, the definition of the damage location was based on three criteria with decreasing importance, see Ramos *et al.* (2010a), that allowed locating all the cracks in the vicinity of the observed experimental positions.



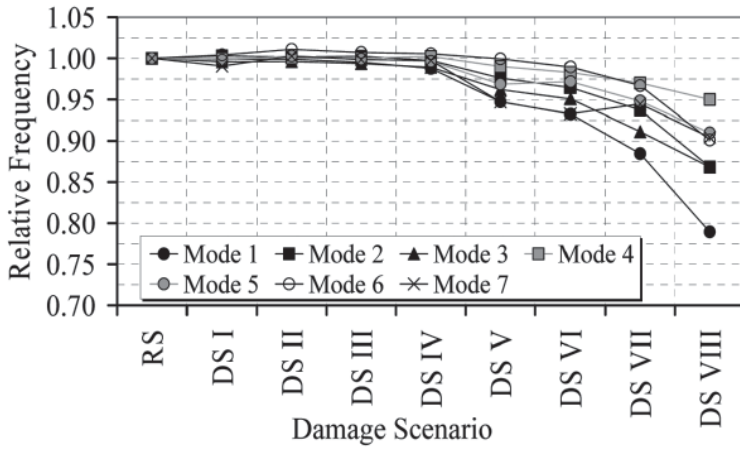


Figure 6 Relative frequency values for ambient excitation.

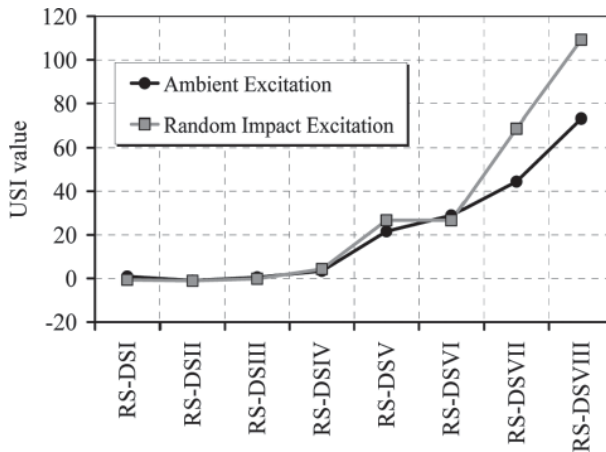


Figure 7 Unified Significance Indicator (USI) results and comparison with the RS.

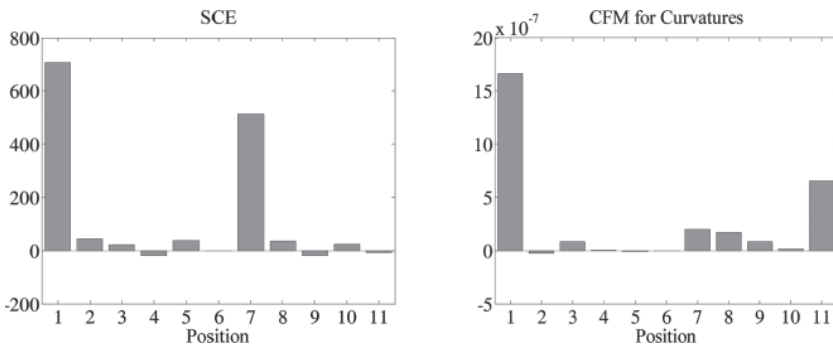


Figure 8 Results with measured curvatures for the comparison between DSIV and DSV.

Finally, with a combination with the Finite Element Model Updating Method, it was possible to conclude that the updating analysis did not provide accurate results, on the contrary to damage analysis using only numerical crack simulation. The difficulties of tuning the numerical model to the experimental mode shapes can be explained by the sensitivity of the dynamic response of the numerical model to the geometry. Another possible explanation for the low quality of the results is the residual deformation of the arch on each static test.

## **MONITORING WITH OPERATIONAL MODAL ANALYSIS: TWO CASE STUDIES USING CONVENTIONAL SENSORS**

The process leading to monitoring of historical masonry structures can be divided in four phases. The first phase is the data collection of the structure, including the historic information, geometrical and topographic survey, damage survey, mechanical materials characterization with non-destructive tests, global dynamic modal test and a numerical model analysis for static and dynamic validation. This is the first approach to the structural behavior in the assumed condition at time “zero”. In the second phase the health monitoring plan can be performed with a limited number of sensors (e.g. a pair of reference accelerometers, strain gauges at critical sections, temperature and humidity sensors, etc). Data should be stored periodically and the monitoring system should be able to send the proper alarms. Environmental effects should be studied and the presence of damage should be observed by the global modal parameters. In the third phase, should it be required by the first two phases, or by a life cycle cost analysis, or by the importance of the structure, a full-scale dynamic survey with more sensors and measuring points should be performed. In this phase the “health condition” of a structure is studied with more detail. Damage identification methods should be applied to the structure after filtering the environmental effects. The aim of the dynamic methods is to confirm and locate the (possible) damage in a global way. Finally, in the last phase, a local approach with visual and complementary non-destructive tests should be performed to locally assess the damage and classify it.

Dynamic identification monitoring system can be used to detect cracks in masonry structures at early stage, the possible breakage or loss of anchorage in a tie, or changes in the boundary conditions, see Ramos et al. (2010b) for more details. Next, two complex case studies are shown, in which the first two phases of the preceding methodology were applied.

### **Mogadouro Clock Tower**

The Mogadouro Clock Tower, see Figure 9, is located inside the castle perimeter of Mogadouro, a small town in the Northeast of Portugal. The tower was built after the year 1559. It has a rectangular cross section of  $4.7 \times 4.5 \text{ m}^2$  and a height of 20.4 m. Large granite stones were used in the corners and rubble stone with thick lime mortar joints were used in the central part of the walls. The thickness of the walls

is about 1.0 m. In 2004, the tower was severely damaged, with by large cracks, material deterioration and loss of material in some parts. A geometrical survey of the structure was performed and the existing damage was mapped. Conservation works carried out in 2005 reinstated the tower safety, including lime grout injection for the consolidation of the walls, replacement of material with high level of degradation, filling of voids and losses, and installation of ties (or a steel belt) at two levels.

Dynamic modal identification tests were performed before and after the works, see Figure 10. The same test planning was adopted in the two conditions by using



Figure 9 Mogadouro Clock Tower and conservation works: (a) before; (b) after.

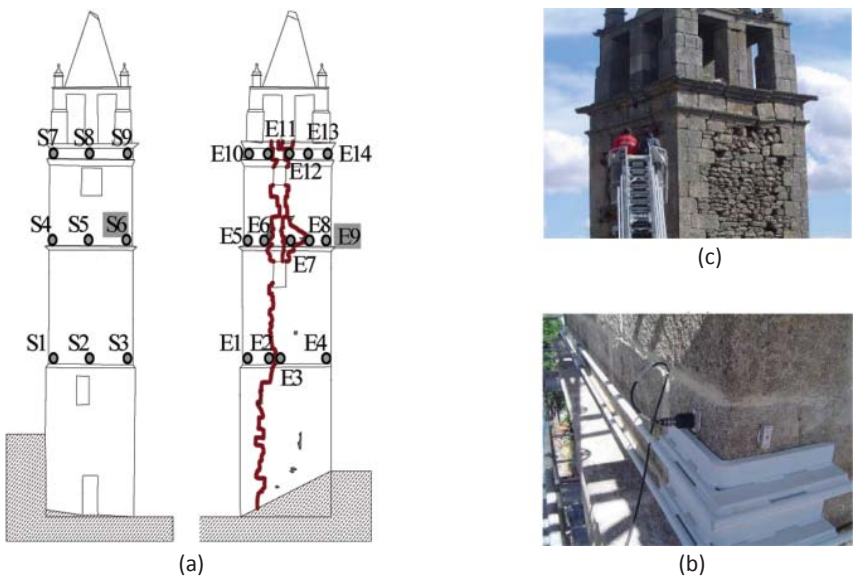


Figure 10 Dynamic tests and examples of sensor locations:  
(a) crack pattern and measuring points in the South and East façades, respectively;  
(b) measurements before rehabilitation works; (c) after rehabilitation works.

the same measuring points. Table 3 presents the first seven estimated natural frequencies and damping ratios and Figure 11a shows selected corresponding mode shapes. An analysis the two structural conditions shows that, on average, the frequencies increased 50% with the works, while the damping decreased 40%. Concerning the modal displacements, local protuberances can be observed in the areas close to the cracks and in the upper part of the tower, before the works. This is due to the presence of severe damage. On the contrary, the structure behaves monolithically after the conservation. Taking into account the previous results, it is possible to conclude that the structure suffered a significant structural intervention and the strengthening works were efficient. One can also conclude that the presence

**Table 3** Mogadouro Clock Tower: Dynamic response before and after the rehabilitation.

Mode Shape	Before		After		$\Delta_{\omega}$ [%]	Before		After		$\Delta_{\xi}$ [%]
	$\omega$ [Hz]	$CV_{\omega}$ [%]	$\omega$ [Hz]	$CV_{\omega}$ [%]		$\xi$ [%]	$CV_{\xi}$ [%]	$\xi$ [%]	$CV_{\xi}$ [%]	
1 <sup>st</sup>	2.15	1.85	2.56	0.21	+19.28	2.68	219.51	1.25	0.13	-53.26
2 <sup>nd</sup>	2.58	1.05	2.76	0.30	+6.70	1.71	94.02	1.35	0.17	-21.00
3 <sup>rd</sup>	4.98	0.69	7.15	0.27	+43.67	2.05	65.33	1.20	0.14	-41.32
4 <sup>th</sup>	5.74	1.56	8.86	0.47	+54.37	2.40	24.27	1.31	0.13	-45.72
5 <sup>th</sup>	6.76	1.13	9.21	0.21	+36.13	2.14	31.74	1.16	0.12	-45.65
6 <sup>th</sup>	7.69	2.94	15.21	2.24	+97.87	2.33	55.98	2.54	0.24	+9.11
7 <sup>th</sup>	8.98	1.21	16.91	1.40	+88.27	2.30	46.39	1.49	0.23	-35.07
Average values	-	1.49	-	0.73	+49.47	2.23	76.75	1.47	0.17	-40.34*

\* - Average value calculated only with negative differences

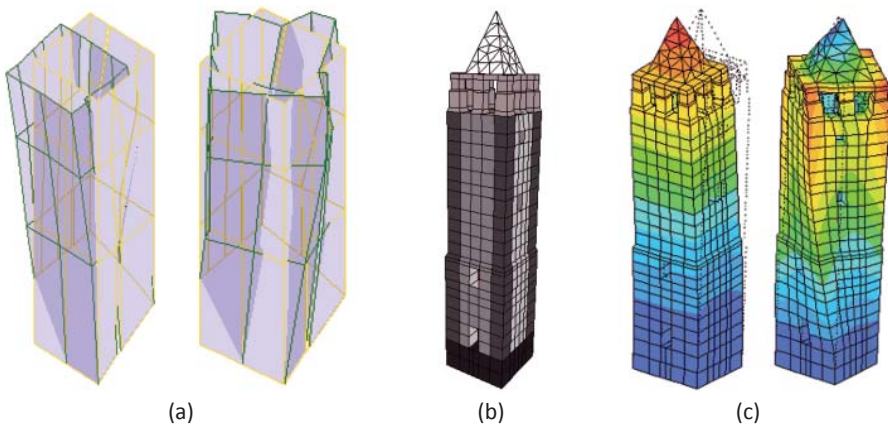


**Figure 11** Mode shapes Mogadouro Clock Tower: (a) measured mode shapes for translation and torsional modes; (b) finite element model, with different masonry qualities for modal updating; (c) tuned numerical mode shapes.

of damage changed the dynamic behavior significantly with respect to the possible original structure. The challenge now is to verify if the cracks were stabilized with the intervention by means of a dynamic monitoring system.

For the structural assessment, a 3D FE model was built. The model updating analysis was performed with the aim to assess the tower dynamic behavior in its actual condition (after the retrofiting). The nonlinear least square method was used to compute the numerical modes. The objective function to be minimized is composed by the residuals formed with calculated and experimental frequencies and mode shapes. The optimization parameters were selected taking into account the possible differences between the material properties and the modulus of elasticity of the different parts was chosen as updating parameters. Figure 11b shows the final 3D model where eight updating parameters can be observed and Figure 11c shows selected tuned modes, which present very good agreement with the experimental ones.

During 2006 and 2007, and after the conservation works, a dynamic monitoring system was installed in the tower. The aim was to evaluate the environmental effects of temperature and relative air humidity on the dynamic behavior of the tower, and to detect any possible non stabilized phenomenon in the structure. Three piezoelectric accelerometers connected to an USB data acquisition card recorded each hour ten minutes of ambient vibrations. In parallel a combined sensor recorded the ambient temperature and relative air humidity. This task was performed in several campaigns (test series), in different periods of the year.

The data series were analyzed and they allowed concluding that the environmental effects significantly change the dynamic response of the structure. Mainly, the water absorption of the walls in the beginning of the raining seasons changes the frequencies about 4%. The significant influence of moisture inside the walls on the dynamic response of masonry structures is not reported in literature, as the changes are always attributed to others environmental effects or loading conditions, such as temperature and excitation level. The series presented in Figure 12 were recorded during October and November, 2006, which is linked to the first strong raining event at the site. As no damage was observed in the structure, the humidity influence can be observed by a shift in the linear relation between frequency and temperature by a transition series.

The ambient temperature, the relative air humidity and the excitation level, by means of the Root Mean Square (RMS) of the signal, were correlated to the resonant frequencies. Multiple linear regression models were compared with Auto Regressive outputs with eXogeneous input models, also known as ARX models, Ljung (1999), in order to evaluate the environmental and loading effects. Figure 13a shows the fitting models through the normalized frequency and simulated errors with the 95% confidence intervals  $c_i$ , and Figure 13b shows the simulated error. In general, the model is able to replicate the frequency variation, but does not takes into account the water absorption phenomenon, because the relative humidity variation does not totally represent that change. The results indicates that ARX models can simulate the

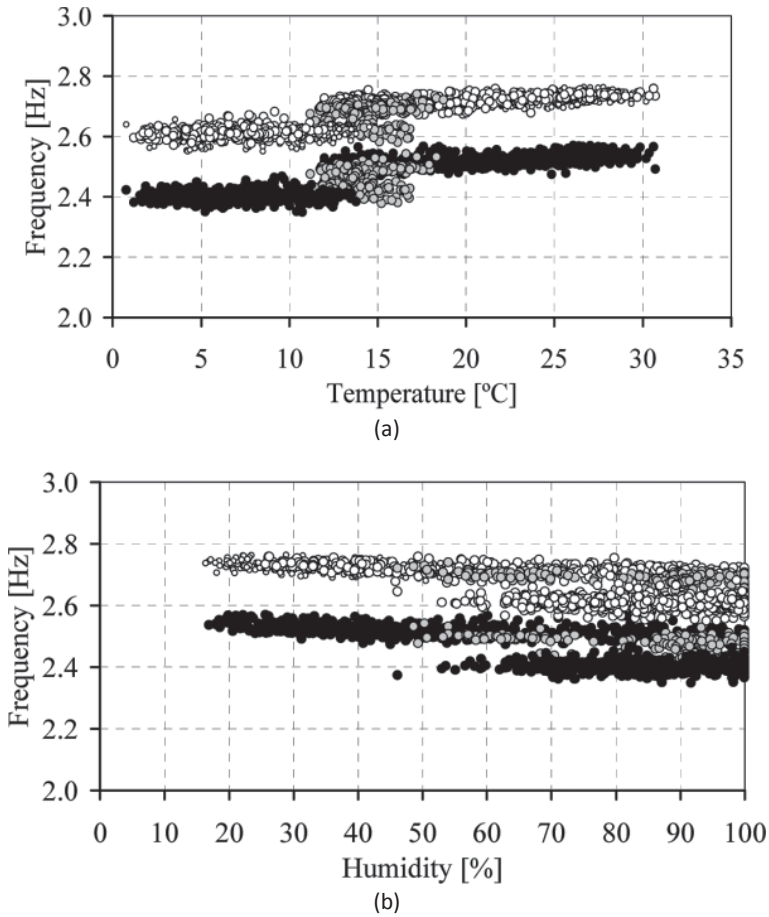


**Figure 12** Environmental effects: (a) temperature; (b) relative air humidity.  
 Note: Black dots correspond to the first frequency, white dots to the second frequency, and grey dots to the transition period of each frequency.

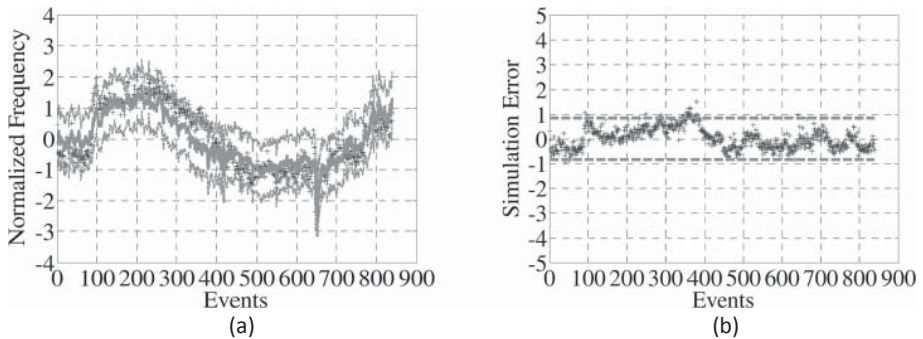


**Figure 13** ARX model  $[3, 2 \ 2 \ 4, 0 \ 0 \ 0]$  for mode shape 1 with 95% confidence intervals: (a) normalized frequency; (b) simulation error.

natural frequencies, but sensors to measure the water absorption inside the walls are necessary in this case to better simulate the dynamic response and to detect the presence of damage. Apparently, no damage was observed by global modal parameters changes during the monitoring period reported.

### Church of Monastery of Jerónimos

The Monastery of Jerónimos, located in Lisbon, is one of the most famous Portuguese monuments, Figure 14. The Portuguese “Manuelino” architectural style of the 16<sup>th</sup> century makes the monument very attractive for tourists. The church of the monastery, Santa Maria de Belém church, has considerable dimensions: a length of 70 m, a width of 40 m and a height of 24 m.

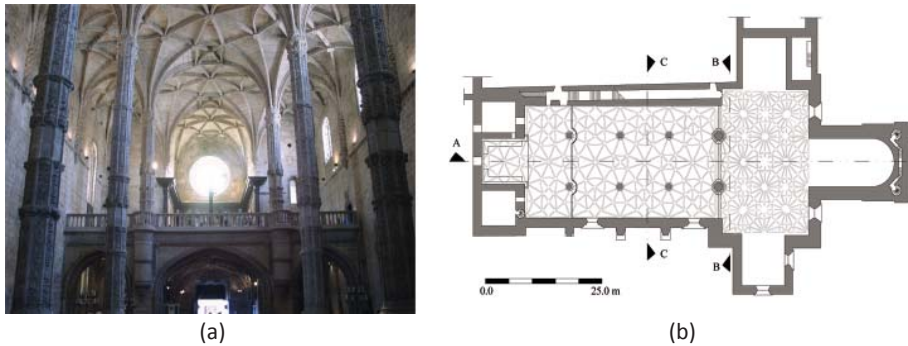


Figure 14 Church of Monastery of Jerónimos: (a) inside view; (b) plan view.

The main nave of the church was tested using output-only modal identifications techniques, which provided the modal parameters: resonant frequencies, mode shapes and damping coefficients. Two techniques were applied to compare the experimental dynamic parameters obtained and have more accurate results. The Enhanced Frequency Domain Decomposition (EFDD), Brincker *et al.* (2000), and the Stochastic Subspace Identification (SSI) method. Thirty points on the top of the main nave were selected to measure the acceleration response. Ten points were located on the top of the external walls with the purpose of measuring the nave boundaries and also the global dynamic response of the church. The other points are located either on the top of the columns or on the top of the vault keys.

Table 4 summarizes six natural frequencies, damping ratios and MAC values estimated by two different output-only system identification techniques. The natural frequencies range from 3.7 to 12.45 Hz and no significant differences could be found between the two methods. For the damping coefficients, differences up to 140% can be observed. The MAC values are only higher than 0.95 for the first two modes as a consequence of the difficulty in exciting this heavy structure. The modes can be found in Ramos *et al.* (2010b).

**Table 4** Monastery of Jerónimos: Comparison of the estimated modal parameters of the main nave.

Mode Shape	$\omega$ [Hz]		$\xi$ [%]		MAC
	EFDD	SSI	EFDD	SSI	
	1 <sup>st</sup>	3.69	3.68	2.34	
2 <sup>nd</sup>	5.12	5.04	1.11	2.68	0.92
3 <sup>rd</sup>	6.29	6.30	1.00	0.82	0.67
4 <sup>th</sup>	7.23	7.29	0.77	1.44	0.67
5 <sup>th</sup>	9.67	9.65	1.10	1.45	0.62
6 <sup>th</sup>	12.45	12.51	1.25	1.19	0.71

Due to the high level of complexity of the structure a beam FE model was manually tuned to the dynamic experimental results. The adoption of a relatively “simple” model is due to the fact that the model is to be used in subsequent non-linear time integration analysis, including a parametric study using a set of mechanical properties, different return period scenarios and strengthening possibilities, see also Roque (2010). The updating parameters were the modulus of elasticity of the columns and the main nave, and the boundary conditions of the columns. The dynamic response is mostly governed by the slender columns, as many local modes appear in the results. The first mode shape of the numerical model is presented in Figure 15.

Since April of 2005, a dynamic monitoring system was installed in the church within the scope of the Euro-Indian research project “Improving the Seismic Resistance of Cultural Heritage Buildings”. The monitoring system is composed of two strong motions recorders (R) with 18 bits AD converters connected to two triaxial force balance accelerometers. One accelerometer (A1) was installed at the base of the structure near the chancel and the other (A2) at the top of the main nave (extrados), between two consecutive columns, and in the location with higher signal levels

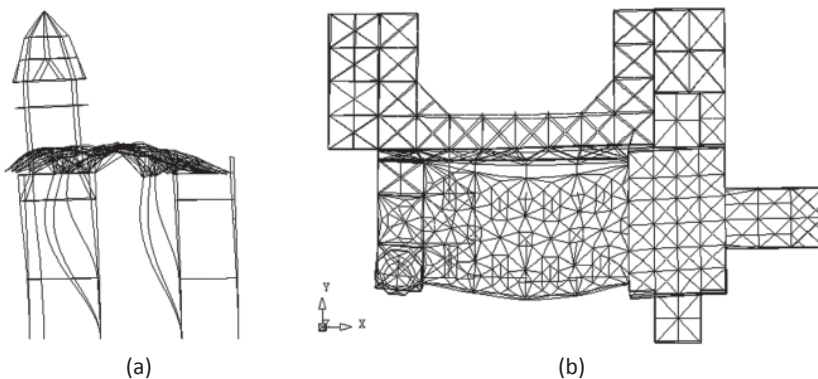


**Figure 15** First mode numerical mode shape at 3.79 Hz: (a) transversal section; (b) plan view.



obtained in the dynamic modal identification analysis. The two recorders are connected by an enhanced interconnection network, which allows a common trigger and time programmed records. The recorder connected to sensor A1 is the master recorder, which enables synchronization and updates the internal clock of the slave recorder connected to sensor A2. The monitoring task is mainly processed by the master recorder, with a trigger armed for low level signals corresponding to micro tremors occurring at the site. In parallel, every month, dynamic data are registered during ten minutes. Also seasonally, to study the environmental effects, ten minutes are recorded every hour during one complete day.

The dynamic monitoring system is complemented by a static one, which measures temperatures and rotation of the columns at several points in the structure. Additional sensors for relative air humidity and wind velocity were recently added to this system. For the study of the environmental and loading effects all data acquired in the strong motion recorders were used. 1300 events were acquired: 28% of which correspond to programmed events with ten minutes of total sampling duration, and 72% correspond to triggered events, with an average sampling duration of one minute and fifteen seconds.

To estimate the modal parameters, the procedure described previously for the Mogadouro Clock Tower was again adopted. It should be stressed that in the modal parameter estimation only the first, the third and the fourth mode shapes of the nave were successful estimated. The majority of the triggered events occurred during working hours, due to the road traffic, special events inside the church (like mass or concerts), and minor earthquakes. With respect to programmed events, it is noted that it was more difficult to estimate the modal parameters during the night period, due to the low ambient excitation level. The results indicate that the temperature effect is significant for the nave. A trend for a bilinear relation between temperature and frequency was found, with an apex for a temperature about 18°C. This trend occurs for all the estimated frequencies.

As no continuum series were recorded in the monitoring system, modeling of thermal inertia is difficult and only static regression models were used. From the observed bilinear trend, two linear regressions for temperature values lower and higher than 17.5°C were adopted. Figure 16a shows the static models for the first estimated

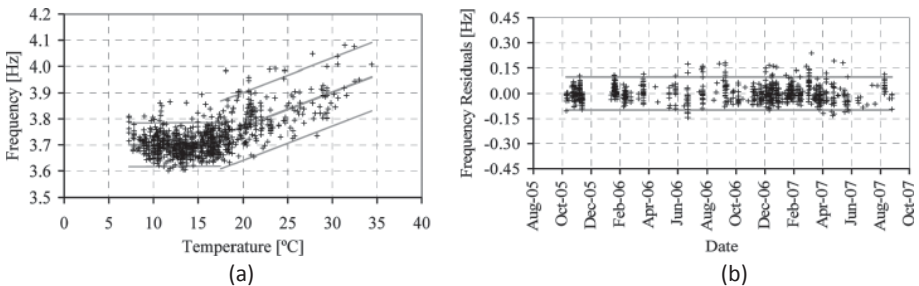


**Figure 16** Static regression for the first mode: (a) temperature influence; (b) residuals history.

frequency by correlating the two quantities, temperature and frequency with the 95% ( $\pm 2\sigma$ ) confidence intervals. The results show that the bilinear static model follows the evolution of the frequencies but a significant number of outliers can be observed in Figure 16b, where the residuals between the first natural frequency and the simulated frequency are shown. This indicates that others environmental effects need to be studied to better model the dynamic response.

Finally, it should be stressed that in 12 February, 2007, at 10:35 am a 5.8 magnitude earthquake, with a Modified Mercalli intensity V, occurred in the Southwest of Lisbon. The permanent staff of the monument felt the ground shake. No visitors were inside the church because on Mondays the church is closed to public. The strong motions recorders acquired the signals and the peak of the frequency contents of the elastic response spectra was in the range of the estimated natural frequencies, but the estimated natural frequencies did not suffer any significant shift, as can be observed through Figure 16b. Therefore, no damage in the structure occurred due to this minor earthquake.

## **OPERATIONAL MODAL ANALYSIS USING COMMERCIAL WIRELESS PLATFORMS**

The research efforts in many scientific areas, such as physics, microelectronics, control, material science, etc., are oriented to the creation of smaller, autonomous and easier to handle mechanisms for sensing purposes. In the area of measuring physical parameters, these goals were successfully achieved via the integration of Micro-Electro-Mechanical Systems (MEMS) with low power and high frequency transceivers, joined in silicon chips. Sensor prototypes, called “motes”, were developed to reach four attributes: sensing, processing, communication and actuation.

A mote is an autonomous, compact device, and a sensor unit that has the capability of processing and communicating wirelessly. One of the biggest strengths of motes is that they can form networks, known as Wireless Sensor Networks (WSN), which allows the units to cooperate between themselves.

Wireless technology is being used for a wide range of applications such as military, environmental monitoring (e.g. indoor for emergency services or outdoor for agriculture applications), support for logistics (e.g. considering the use of wearable motes in firemen), human centric (motes for health science and health care) and robotics. The use of wireless technology with embedded MEMS for structural monitoring was first proposed by Kiremijidian *et al.* (1997), aiming at the integration of wireless communications with sensors in order to develop a near real time monitoring system. After these preliminary studies, many efforts to improve the technology had been carried out. The first case of study in which wireless based systems were used to monitor civil engineering structures, was the Alamosa Canyon Bridge in 1998, Straser and Kiremijidian (1998). Due to fact that masonry structures are difficult to excite and due to the low resolutions capabilities of the commercial

**Table 5** Characteristics of a MEMS and a conventional piezoelectric accelerometer.

	MEMS microaccelerometer	Piezoelectric accelerometer
Sensor Type	ADXL202JE	PCB 393B12
Channels	X, Y	X
Range (g)	$\pm 2.0$	$\pm 0.5$
Sensitivity (mV/g)	167 $\pm 17\%$	10000
Resolution (g rms)	0.002	0.000008
Size (mm)	5.0 x 5.0 x 2.0	30.2 (diam.) x 55.6 (high)
Weight (gram)	1.6	210.0

MEMS, only one application was found, namely the Aquila Tower in Italy, see Ceriotti et al. (2009).

The conventional wired based sensors used here were the high sensitivity piezoelectric accelerometers model PCB 393B12. For DAQ purposes, the NI-USB9233 board with an ADC resolution of 24 bits was selected. In the case of the wireless based systems, the Crossbow technology was chosen, as it offers inexpensive solutions with low powering boards and platforms with embedded microaccelerometers. For comparison purposes Table 5 presents the characteristics of the microaccelerometer ADXL202 embedded in the Crossbow platforms and the piezoelectric accelerometer PCB 393B12.

### Dynamic Response of an Inverted Pendulum

A Single Degree-of-Freedom (SDOF) structure represented by an inverted pendulum is one of the simplest examples used by civil engineers to explain the fundamentals of structural dynamics. In this work, this pendulum is also used to evaluate and understand the behavior of commercial wireless-based platforms and their use for civil engineering works. The studied specimen was an inverted timber pendulum with 1.70 m high and with steel plates in its top and base (Figure 17). To perform a complete dynamic characterization of the pendulum, three wire based and three wireless with embedded MEMS platforms accelerometers were used (the MEMS sensors were programmed to perform measurements only in one axis). These sensors were arranged in two setups keeping the node 1 as common for both measurements. For comparison purposes the wired and wireless systems were set to run concurrently. Initially, the performance with respect to an acceleration time series was studied using tests under random excitation and ambient noise. Figure 18 shows the recorded signal by mote 3 and accelerometer 3 in both scenarios. The results demonstrate the poor performance of the micro accelerometers for measuring low amplitude vibrations. The maximum values and the root mean square (RMS) registered by the wireless platforms are, respectively, 3 to 6 times and 8 to 22 times lower than the values recorded by the conventional platforms with ambient noise. Similar results were obtained in the case of the RMS in random excitation, even if the time series recorded with both systems are rather similar.

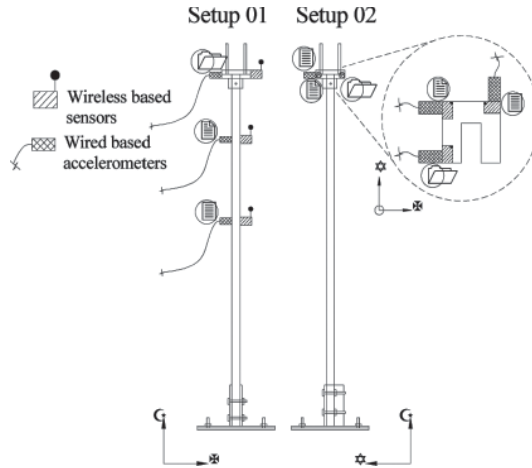


Figure 17 Experimental modal analysis of a laboratory specimen, with setup description.

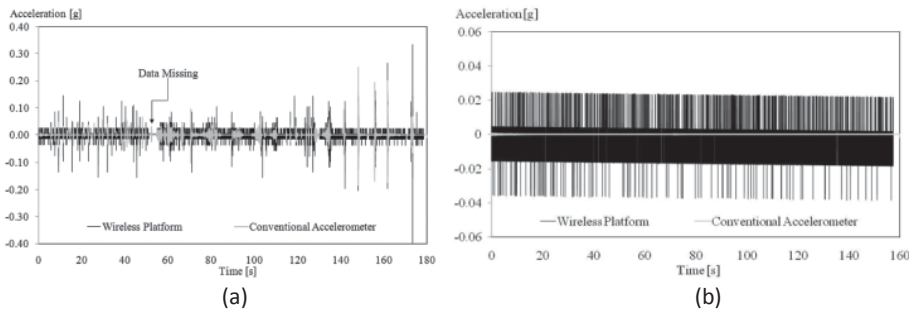


Figure 18 Time series collected by mote 3 and accelerometer 3 in the inverted pendulum tests: (a) response under random excitation in Setup 01; (b) response under ambient noise in Setup 02.

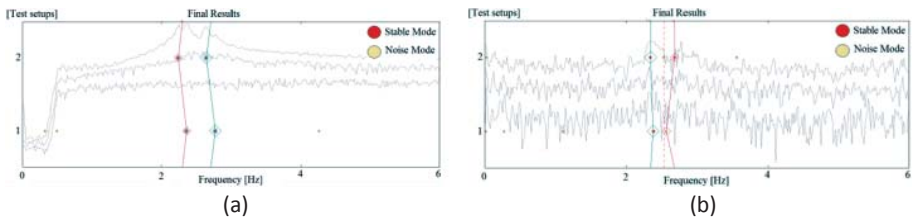


Figure 19 Stabilization diagrams for the analysis of the time series recorded under random excitation in the inverted pendulum tests: (a) results of the conventional wired based accelerometers; (b) results of the wireless platforms.

**Table 6** Results of the experimental modal analysis of the inverted pendulum study.

	Mode	Conventional Accelerometers		Wireless Platforms			
		$f$ (Hz)	$\xi$ (%)	$f$ (Hz)	$\xi$ (%)	$f_{Error}$ (%)	$\xi_{Error}$ (%)
Random excitation	1	2.30	1.45	2.35	3.57	2.13	59.39
	2	2.71	1.57	2.68	2.94	1.12	46.60
Ambient	1	2.26	0.82	2.41	9.82	6.22	--
	2	2.63	2.12	2.83	10.42	7.07	--

Then, the dynamic characteristics of the system were studied. For this purpose, the SSI-Data method implemented in the ARTeMIS extractor software was used. Figure 19 shows the stabilization diagram corresponding to the random excitation and Table 6 shows a summary of the results accelerometers, where  $f$  is the frequency and  $\xi$  is the damping. According to the frequency content results, the wireless based platforms give accurate results (errors of about 2% for random excitation and about 7% for ambient vibration). When the structure is lightly and randomly excited, the modal identification is easier because the stable poles are properly aligned in the natural frequencies. In the case of ambient noise the dynamic identification becomes more complicated due to the appearance of noise poles (stabilization diagrams not shown). The results related to damping tend to show a large scatter and are often unreliable. Still, no correlation was found between damping values using conventional and wireless based systems, with extremely large (and incorrect) values found with the wireless based platforms. Due to the lack of synchronization algorithms implemented for the motes, no information can be gathered on the mode shapes. A prototype wireless sensor with synchronization was developed in Aguilar (2010).

### The Chimneys at Paço dos Duques, Guimarães

The Paço dos Duques (Palace of the Dukes of Bragança) was built between 1422 and 1433 by D. Afonso in Guimarães, north of Portugal, see Figure 20. One of the most important changes in the structure of the building was the addition of chimneys in the roof. The original building had only four chimneys and, in the intervention started in 1937, 34 more chimneys were added. Since 2002, the building suffered some conservation works, mostly related to the roofs and chimneys. The chimneys exhibited considerable damage, with one chimney requiring strengthening.

Based on the previous results of the experimental tests, the use of commercial wireless platforms for structural dynamic monitoring was again explored. The dynamic response of one of the four original chimneys was studied using conventional and wireless platforms. Figure 21a shows a general view of the conservation works that were carried out and Figure 21b shows the location of the wireless platforms in the experimental tests.



**Figure 20** Palace of the Dukes of Bragança (“Paço dos Duques”), in Guimarães.



**Figure 21** Chimneys at Paço dos Duques: (a) recent conservation works; (b) sensors location.

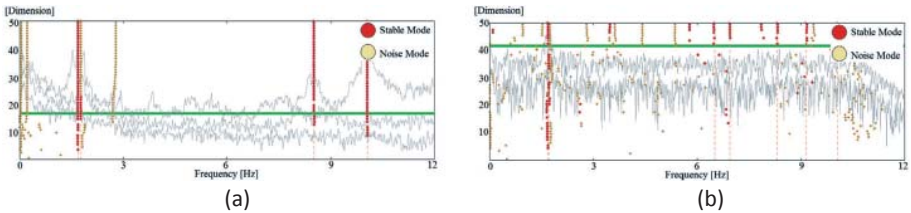


**Figure 22** Stabilization diagrams of the analysis of the time series recorded under random excitation in the chimney at Paço dos Duques tests: (a) results of the conventional wired based accelerometers; (b) results of the wireless platforms.

**Table 7** Dynamic response of the chimney at Paço dos Duques.

Mode	Conv. Accelerometers		Wireless Platforms			
	$f$ (Hz)	$\xi$ (%)	$f$ (Hz)	$\xi$ (%)	$f_{Error}$ (%)	$\xi_{Error}$ (%)
1	1.69	1.34	1.68	1.61	0.60	16.77
2	1.77	4.22	1.71	0.72	3.51	--

The advantages of using wireless platforms were clear in this case study, as their use is much simpler. The DAQ process was also easier allowing safer work in a zone with difficult access. Figure 22 shows the stabilization diagrams of the analysis of the time series recorded under random excitation. Table 7 shows the results of the identified frequencies using conventional accelerometers and wireless platforms. The results show very small differences in the identified frequencies obtained by using the conventional and the wireless platforms (maximum error is 3.5%). Again, inconclusive results are obtained with respect to damping. When the tests are performed with ambient noise (results not shown) similar frequencies could be identified, again with more difficulties due to the spurious poles appearing in the stabilization diagrams.

## **CONCLUSIONS**

A damage identification approach was proposed based on vibrations measurements for masonry structures and a selection of methods available in the literature. The methods were combined in a qualitative way with the aim to capture the difficult phenomena and in assisting the decision of damage identification analysis. The methods can be easily applied to masonry structures and they give information about the detection (Level 1), the localization (Level 2) and, possibly, the assessment (Level 3) of damage.

A methodology based on operational modal analysis was presented for masonry structures, aiming at detecting damage at an earlier stage. The methodology comprises four phases, namely data collection, simplified health monitoring, detailed health monitoring and local non-destructive testing. As an illustration, the first two phases were applied to two complex Portuguese monuments using conventional sensors. For these monuments, the modal identification results, the development of structural model with model updating techniques, for subsequent assessment with FE models, the installation of monitoring systems and the automatic parameter retrieval were presented. From the experience with the two cases, the proposed methodology for damage identification seems to be useful and applicable to masonry structures, especially to complex historical constructions. In particular, the frequency monitoring seems to be a reliable quantity for damage detection.

A new platform for performing operational modal analysis of structures, based on wireless technology with embedded MEMS sensors, was also tested. Commercial WSN platforms available in the market were chosen for comparison purposes against widely used conventional wired based systems. The results showed that the WSN platforms have poor performance with respect to the acceleration time series recorded, due to the low resolution of the microaccelerometers and DAQ systems embedded. The wireless platforms showed also very poor performance for the detection of modal shapes due to the lack of synchronization algorithms. In the case of frequency detection, reliable results were obtained especially when the systems were randomly excited. Synchronization is needed, and a prototype is available from Aguilar (2010), for modal shape identification. Still, ambient vibration tests of stiff structures remains a challenge for WSN platforms.

## References

- Aguilar, R. (2010), Dynamic structural identification using Wireless Sensor Networks, PhD Thesis, University of Minho, Portugal. Available from [www.civil.uminho.pt/masonry](http://www.civil.uminho.pt/masonry).
- Brincker, R., Zhang, L., Andersen, P. (2000), Modal Identification from Ambient Responses using Frequency Domain Decomposition, Proceedings of the 18th International Seminar on Modal Analysis, San Antonio, Texas, 7-10 February.
- Cerioti, M., Mottola, L., Picco, G.P., Murphy, A.L., Guna, S., Corra, M., Pozzi, M., Zonta, D., Zanon, P. (2009), Monitoring Heritage Buildings with Wireless Sensor Networks: The Torre Aquila Deployment. International Conference on Information Processing in Sensor Networks-IPSN09, San Francisco, USA.
- Chang, P.C., Flatau, A., and Liu, S.C. (2003), Review Paper: Health Monitoring of Civil Infrastructure, *Structural Health Monitoring*, 2(3), p. 257-267.
- Doebling, S.W., Farrar C.R., Prime, M.B., and Shevitz D. (1996), Damage identification and health monitoring of structural and mechanical systems from changes in their vibration characteristics: a literature review, Los Alamos National Laboratory, NM, 132 pp.
- Kiremijidian, A.S., Straser, E.G., Meng, T.H., Law, K, Soon, H. (1997), Structural Damage Monitoring for Civil Structures. International Workshop - Structural Health Monitoring, p. 371–382.
- Ljung, L. (1999), System Identification: Theory for the User, Second edition, Prentice Hall, Upper Saddle River, NJ, USA.
- Lourenço, P.B. (2002), Computations of historical masonry constructions, *Progress in Structural Engineering and Materials*, 4(3), p. 301-319.
- Lourenço, P.B., Milani, G., Tralli, A., Zucchini, A. (2007), Analysis of masonry structures: review of and recent trends of homogenisation techniques, *Canadian Journal of Civil Engineering*, 34 (11), p. 1443-1457
- Lourenço, P.B., Mendes, N., Ramos, L.F., Oliveira, D.V. (2011), On the analysis of masonry structures without box behavior, *International Journal of Architectural Heritage*, 5(4), pp. 367-390.
- Lynch J.P. (2007), An overview of wireless structural health monitoring for civil structures, *Journal of Philosophical Transactions of the Royal Society of London Series A, Mathematical and Physical Sciences*. p. 345-372.
- Maeck, J. (2003), Damage Assessment of Civil Engineering Structures by Vibration Monitoring, PhD Thesis, Catholic University of Leuven, Belgium.
- Peeters, B. (2000), System identification and damage detection in civil engineering, PhD Thesis, Catholic University of Leuven, Belgium.
- Ramos, L.F. (2007), Damage Identification on Masonry Structures Based on Vibration Signatures, PhD Thesis, University of Minho, Portugal. Available from [www.civil.uminho.pt/masonry](http://www.civil.uminho.pt/masonry).
- mos, L.F., De Roeck, G., Lourenço, P.B., Campos-Costa, A. (2010a), Damage identification on arched masonry structures using ambient and random impact vibrations, *Engineering Structures*, 32(1), p. 146-162.
- Ramos, L.F., Marques, L., Lourenço, P.B., De Roeck, G., Campos-Costa, A., Roque, J. (2010b), Monitoring of Historical Masonry Structures with Operational Modal Analysis: Two Case Studies, *Mechanical Systems and Signal Processing*, 24(5), p. 1291-1305.
- Ramos, L.F., Aguilar, R., Lourenço, P.B. (2010c), Operational modal analysis of historical constructions using commercial wireless platforms, *Structural Health Monitoring* (accepted for publication), doi: 10.1177/1475921710388973.
- RaRoque, J.C.A. (2010), Metodologia integrada para avaliação e mitigação da vulnerabilidade sísmica das construções históricas em alvenaria. A igreja dos Jerónimos como caso de estudo, PhD Thesis, University of Minho, Portugal. Available from [www.civil.uminho.pt/masonry](http://www.civil.uminho.pt/masonry).
- Straser, E.G., Kiremijidian, A.S. (1998), A Modular Wireless Damage Monitoring System for Structures. *The John A. Blume Earthquake Engineering Center*, 128.